

Spatiotemporal variability and change in rainfall in the Oti River Basin, West Africa

Daniel Kwawuvi ^{a,*}, Daouda Mama^b, Sampson K. Agodzo^c, Andreas Hartmann^{d,f}, Isaac Larbi^e, Enoch Bessah ^c, Andrew Manoba Limantol^e, Sam-Quarcoo Dotse ^e and GniPGA Issoufou Yangouliba^a

^a Climate Change and Water Resources, West African Science Service Centre on Climate Change and Adapted Land, Use (WASCAL), Université d'Abomey Calavi, Cotonou 03 BP 526, Benin

^b Institut National de l'Eau, Université d'Abomey-Calavi, Cotonou 03, Benin

^c Department of Agricultural and Biosystems Engineering, Kwame Nkrumah University of Science and Technology, PMB, Kumasi, Ghana

^d Chair of Hydrological Modeling and Water Resources, University of Freiburg, Freiburg im Breisgau, Germany

^e School of Sustainable Development, University of Environment and Sustainable Development, PMB, Somanya, Ghana

^f Institute of Groundwater Management, Technical University of Dresden, Dresden, Germany

*Corresponding author. E-mail: kwawuvi.d@edu.wascal.org, danielkwawuvi@gmail.com

 DK, 0000-0002-5068-3386; EB, 0000-0002-2187-2022; S-QD, 0000-0002-1168-2209

ABSTRACT

Understanding rainwater dispersion in a spatiotemporal context is invaluable toward resourceful water management and a food-secure society. This study, therefore, assessed the variations in rainfall at a spatiotemporal scale in the Oti River Basin of West Africa for observed (1981–2010) and future periods (2021–2050) under the representative concentration pathways (RCPs) 4.5 and 8.5 emission scenarios. Rainfall data from meteorological stations and Climate Hazards Group Infrared Precipitation with Stations (CHIRPS) were used. The percentage changes in rainfall for the peak month as well as for rainy and dry seasons under the two climate scenarios were determined. The coefficient of variation (CV) and the standardized anomaly index (SAI) were used to assess annual variations in rainfall. In general, under both emission scenarios, rainfall is projected to decrease over the study area. However, the amount of rainfall during the peak month (August) for RCP4.5 and RCP8.5 could increase by 0.26 and 9.3%, respectively. The highest SAIs for the observed period were +1.58 (2009) and –2.29 (1983) with the latter showing a relationship with historic drought in the basin. The projected SAI under RCP4.5 and RCP8.5 indicated extremely wet (+2.12) and very wet (+1.91) periods for the years 2037 and 2028, respectively. The study provides relevant information and a chance to aid the design of innovative adaptation measures toward efficient water management and agricultural planning for the basin.

Key words: climate, Oti River Basin, rainfall, spatiotemporal distribution, variability, West Africa

HIGHLIGHTS

- Spatiotemporal rainfall analysis was conducted over the Oti River Basin.
- The performance of climate models is improved when bias-corrected.
- Rainfall is projected to decrease in the basin.
- The decline in rainfall poses a threat to the livelihood of fringed communities.
- The Mann–Kendall test fostered knowledge of rainfall trends in the basin.

INTRODUCTION

Sustainable management of water resources, agricultural production and all hydro-ecological services at a river basin level is directly linked to empirical knowledge of the distribution of rainfall in space and time over the basin. Understanding climatic conditions, particularly spatiotemporal distribution of rainfall, is therefore vital for natural resources management in developing countries as in Africa with rising population growths and weak responsive capacity to climate change and variability impacts (Ampadu 2021).

With significant rainfall variability in time and space, West Africa is sensitive to extreme droughts and flooding due to climate change (Lebel *et al.* 2009). This is due to an undeviating relationship between rainfall and global climate (Twisa & Buchroithner 2019; Nhemachena *et al.* 2020). The variability of rainfall has caused lengthy droughts and floods in most parts of West Africa, posing a serious threat to the region. The savannah and semiarid areas, since the 1960s, have recorded

This is an Open Access article distributed under the terms of the Creative Commons Attribution Licence (CC BY 4.0), which permits copying, adaptation and redistribution, provided the original work is properly cited (<http://creativecommons.org/licenses/by/4.0/>).

events of famines and floods (Epule *et al.* 2017). Regrettably, climate variability is likely to intensify (Suleiman & Ifabiye 2015), thereby making rainfall in the Sahel region increasingly unpredictable (IPCC 2014). When the climate changed in the 1960 and 1970s, rainfall was said to have decreased by 15 and 30%, respectively (Oguntunde *et al.* 2006). The 1980s have been regarded as West Africa's driest decade of the 20th century (Nicholson & Palao 1993).

Kasei *et al.* (2010) studied drought recurrence across the Volta Basin and found that the severity was below -2.0 , which affected almost 75% of the area. This means that most of the areas in the basin suffered from drought in 1961, 1970, 1983, 1992 and 2001. On the other hand, the Oti River Basin (ORB) has experienced flood situations in 1998, 2007, 2008, 2010 and 2018, resulting in massive human deaths and infrastructural damage (Tschakert *et al.* 2010; Komi *et al.* 2016). The recorded damage during flooding episodes shows the extent to which the basin-dependent countries are exposed. Regarded as the worst flood ever faced in the basin was that of 2007, which killed 23 people in Togo, 46 in Burkina Faso and 56 in Ghana (Tschakert *et al.* 2010; Komi *et al.* 2016).

Water and agriculture sectors are key to the actualization of sustainability and economic growth within the region; however, their regular susceptibility toward the changing climate makes it difficult to achieve sustainable development (Hope 2009; Chemnitz & Hoeffler 2011; Nhemachena *et al.* 2020). Alterations in climate have been seen as a major challenge to agriculture and food sufficiency in Africa, especially in rainfed agriculture-dependent regions like West Africa (Wheeler & Von Braun 2013). Agriculture in the West African region represents around 95% of the arable land, engages around 65% of workers and augments the region's economy by 30–70% (Blanc 2012; Akumaga & Tarhule 2018). Kasei *et al.* (2010) have opined that the high irregularity in rainfall amounts, as well as spatiotemporal patterns in the ORB, are the main reasons for food production changes, particularly in the basin's northern sections.

Considering the critical role that rainfall plays in the economies of the countries in the basin, water resource authorities and the agricultural sector have to deal with issues relating to rainfall fluctuations on a regular basis. Accordingly, adjusting to this climatic fluctuation is a key component of reducing climatic shocks in the basin-dependent countries (Nhemachena *et al.* 2020). Therefore, a close monitoring of the present and future amount of rainfall and its variations would be useful for managing water and agronomic scheduling over the ORB.

Moreover, different studies have been conducted on the Volta Basin and some parts of the ORB with only scarce station data with no full focus on the main ORB. Kasei *et al.* (2010), for instance, explored the yearly rain deficiency over the Volta Basin. Komi *et al.* (2017) modeled the extent of flood hazard in the Togo part of the ORB. Klassou & Komi (2021) also analyzed extreme rainfall over the middle part of the ORB and focused on some selected extreme indices. Badjana *et al.* (2014) also probed the changes in land cover in the Kara basin, a sub-basin of the ORB. The present study uses both observed data from meteorological stations and Climate Hazards Group Infrared Precipitation with Stations (CHIRPS) data (Funk *et al.* 2015) to analyze rainfall changes within the ORB. The objective of this study is therefore to analyze the spatiotemporal variability and change in rainfall over the ORB for an understanding of the distribution of rainfall in space and time as vital empirical evidence for sustainable management of water resources and agricultural production in the basin.

METHODS

Study area

The geographical location of the ORB is found within four West African nations (Ghana, Burkina Faso, Togo and Benin) and lies between longitudes 6°W and 2°E and latitudes 0° and 15°N (Figure 1). It has an estimated surface area coverage of around 72,000 km², and it is a sub-basin of the Volta basin system in West Africa (Barry *et al.* 2005; Kasei 2009). The movement and interactions of the Inter-Tropical Discontinuity (ITD) and the associated West African Monsoon govern the basin's climate. Annual rainfall ranges from 1,100 mm (north) to 1,400 mm (south), with pan evaporation of about 2,540 mm/year and runoff of approximately 254 mm/year (Kasei 2009). The basin experiences a single rainfall pattern, having its maximum rain in August. The rainy season lasts from April to October, while the dry season lasts from November to March (Klassou & Komi 2021). The average annual temperature ranges from 25.9 to 34 °C. Because the basin's topography is steep and rainfall is quite high, surface runoff is facilitated, resulting in around 25% of the yearly total flow contributions to the Volta Lake (Barry *et al.* 2005).

Station and satellite climate dataset

Daily rainfall data for eight climate stations within the Oti basin for the period 1981–2010 were acquired from the Ghana Meteorological Agency, the National Meteorological Service of Togo and the Benin Meteorological Department. Additionally, due to the limited spatial allocation of weather stations, gridded daily rainfall data for 22 gridded points were sourced

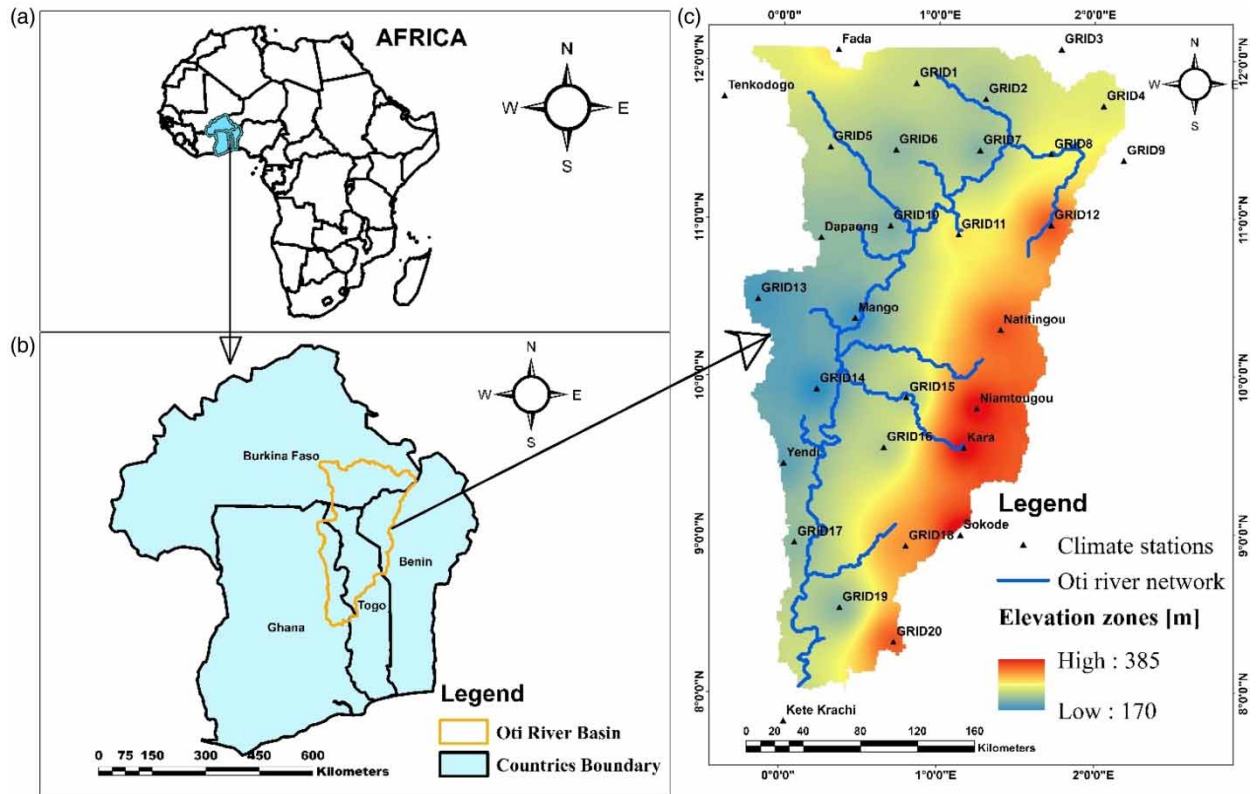


Figure 1 | Map of study area showing (a) the location of Oti Riparian countries in Africa highlighted, (b) the ORB (highlighted in yellow) shared by Ghana, Burkina Faso, Togo and Benin and (c) digital elevation model, climate stations and river network in the ORB. Please refer to the online version of this paper to see this figure in color: <http://dx.doi.org/10.2166/wcc.2022.368>.

from CHIRPS, as presented in Table 1 and shown in Figure 1. Daily rainfall CHIRPS data were extracted in R software (Packages: *ncdf4* and *raster*) applying respective locations of the 22 gridded points for 1981–2010. Several research studies (e.g., Dembélé *et al.* 2020; Muthoni 2020; Satgé *et al.* 2020) have applied CHIRPS in both the Volta basin and the West African region and have proven that it can accurately estimate station data, and therefore the CHIRPS data can be used in place of station data.

Climate models' datasets

The study used rainfall simulations from global circulation models (GCMs) under the Coordinated Regional Climate Downscaling Experiment (CORDEX-Africa) (Samuelsson *et al.* 2011; Kjellström *et al.* 2016). The GCMs were downscaled by the Rossby Centre regional atmospheric model (RCA4) at a spatial resolution of $0.44^\circ \times 0.44^\circ$ ($\sim 50 \text{ km} \times 50 \text{ km}$). Table 2 shows the climate models and the institute that created them. The GCMs-RCMs were selected because they have been widely used across the Volta basin (e.g., Kunstmann & Jung 2005; Annor *et al.* 2017). In addition, Akinsanola *et al.* (2017) and Agyekum *et al.* (2018) used these GCMs to evaluate rainfall simulations over West Africa and have attested to their suitability. The study considered climate change datasets under representative concentration pathways (RCPs) 4.5 and 8.5 for the future period 2021–2050.

Quality control, performance evaluation and bias-correction of RCMs

Using Microsoft Excel and Rclimdex package, the study checked for data quality for the eight stations (Natitingou, Kete-Krachi, Yendi, Dapaong, Kara, Mango, Niamtougou and Sokode). The CHIRPS rainfall data were used to accurately fill rainfall data gaps detected in the Kete-Krachi (1–30 June 1984) and Niamtougou (2006) (see Aguilar *et al.* 2009; Larbi *et al.* 2018).

To evaluate the efficiency of the RCMs, the simulated historical rainfall was compared with the observed rainfall at the mean monthly scale using the Taylor diagram. The performance evaluation was done at a monthly scale because it best shows the characteristics of rainfall change (Gulacha & Mulungu 2016). The commonly used statistical measures like Pearson's correlation coefficient (r), standard deviation and root-mean-square error (RMSE) were employed to evaluate the

Table 1 | Observed and virtual climate locations (1981–2010)

Stations	Longitude (°)	Latitude (°)	Data type	Relative location
GRID1	0.85	11.86	Gridded	Upper basin
GRID2	1.30	11.76	Gridded	Upper basin
GRID3	1.78	12.08	Gridded	Upper basin
GRID4	2.06	11.72	Gridded	Upper basin
GRID5	0.31	11.45	Gridded	Upper basin
GRID6	0.73	11.44	Gridded	Upper basin
GRID7	1.26	11.44	Gridded	Upper basin
GRID8	1.72	11.41	Gridded	Upper basin
GRID9	2.19	11.37	Gridded	Upper basin
GRID10	0.69	10.96	Gridded	Upper basin
GRID11	1.13	10.90	Gridded	Upper basin
GRID12	1.72	10.96	Gridded	Upper basin
GRID13	-0.15	10.49	Gridded	Middle basin
GRID14	0.23	9.92	Gridded	Middle basin
GRID15	0.80	9.87	Gridded	Middle basin
GRID16	0.66	9.55	Gridded	Middle basin
GRID17	0.09	8.95	Gridded	Lower basin
GRID18	0.80	8.93	Gridded	Lower basin
GRID19	0.38	8.54	Gridded	Lower basin
GRID20	0.73	8.32	Gridded	Lower basin
Natitingou	1.40	10.30	Station	Middle basin
Fada	0.35	12.07	Gridded	Upper basin
Tenkodogo	-0.38	11.77	Gridded	Upper basin
Kete-Krachi	0.03	7.82	Station	Lower basin
Yendi	0.02	9.45	Station	Lower basin
Dapaong	0.25	10.88	Station	Upper basin
Kara	1.17	9.55	Station	Middle basin
Mango	0.47	10.37	Station	Middle basin
Niamtougou	1.25	9.80	Station	Middle basin
Sokode	1.15	9.00	Station	Lower basin

effectiveness of the RCMs. The position of each model and the ensemble mean in the acceptable range of the statistical measures [$r=-1$ to 1) and (RMSE= $0-\infty$, with 0 being the perfect fit)] showed how well it simulates rainfall in the basin (Moriassi *et al.* 2007; Dembélé & Zwart 2016; Bessah *et al.* 2020).

The simulated daily rainfall dataset in this study was extracted and bias-corrected using the CMhyd application. The bias-correction method employed was the quantile-quantile mapping technique (Boé *et al.* 2008; Johnson & Sharma 2011). The CMhyd took the observed and the simulated rainfall data (thus, the historical and future scenarios) and used the overlapping period 1981–2005 to calculate the correction parameters for the future period (2021–2050) under RCP4.5 and RCP8.5 scenarios. The bias-correction technique helps to adjust the simulated RCM climate values to fall in line with the observed (Teutschbein & Seibert 2012). The procedure for the bias-correction as demonstrated in Thom (1958) is as follows:

$$P_{contr}^*(d) = F_{\gamma}^{-1}(F_{\gamma}(P_{contr}(d)|\alpha_{contr,m},\beta_{contr,m})|\alpha_{obs,m},\beta_{obs,m}) \quad (1)$$

$$P_{scen}^*(d) = F_{\gamma}^{-1}(F_{\gamma}(P_{scen}(d)|\alpha_{contr,m},\beta_{contr,m})|\alpha_{obs,m},\beta_{obs,m}) \quad (2)$$

Table 2 | Description of Climate Model Intercomparison Project 5 GCMs downscaled by RCA4

GCM name	Short name	Institution	Country
CCCma-CanESM2	CanESM2	Canadian Centre of Climate Modelling and Analysis	Canada
CNRM-CERAFACS- CNRM-CM5	CNRM-CM5	Centre National de Recherches Météorologiques-Groupe d'études de l'Atmosphère Météorologique and Centre Européen de Recherche et de Formation Avancée	France
ICHEC-EC-EARTH	EC-EARTH	Consortium of European research institution and researchers	Europe
IPSL-IPSL-CM5A-MR	IPSL-CM5A-MR	Institut Pierre-Simon Laplace	France
MIROC-MIROC5	MIROC5	National Institute for Environmental Studies, and Japan Agency for Marine- Earth Science and Technology	Japan
MPI-M-MPI-ESM-LR	MPI-ESM-LR	Max-Planck-Institut für Meteorologie (Max-Planck Institute for Meteorology)	Germany
NCC-NorESM1-M	NorESM1-M	The Norwegian Climate Center	Norway
NOAA-GFDL-GFDL- ESM2M	GFDL-ESM2M	NOAA Geophysical Fluid Dynamics laboratory	USA

NB: Models hereafter shall be referred to by the short names in Table 2.

where P_{contr}^* is the corrected value for the RCM control run (1981–2005) for the day d , with month m , P_{scen}^* is the simulated rainfall under historical climate scenario, F_γ is the Gamma cumulative distribution function, α is the shape parameter and $\beta_{obs,m}$ is the scale parameter for the month.

Rainfall trend and variability analysis

To explore the occurrence of rainfall in the ORB, the monthly rainfall analysis was conducted for both the observed (1981–2010) and future periods (2021–2050) under RCP4.5 and RCP8.5 scenarios. The percentage change in rainfall for the peak month (August) under the future scenarios was computed relative to the observed. Also, the amount and rate change in rainfall for rainy and dry seasons were determined.

Variations and trends in rainfall at an annual scale for the historical period (1981–2010) and the future period (2021–2050) under RCP4.5 and RCP8.5 scenarios were analyzed using the coefficient of variation (CV) and the standardized anomaly index (SAI).

The CV was computed using the following formula:

$$CV = \frac{\sigma}{\mu} \times 100 \quad (3)$$

where σ is the standard deviation and μ is the mean rainfall for the temporal scales used. The degree of rainfall variations were low ($CV < 20$), moderate ($20 < CV < 30$) and high ($CV > 30$) (Alemu & Bawoke 2019).

The SAI of rainfall was calculated using the following equation:

$$SAI_i = \frac{X_i - \bar{X}}{\sigma} \quad (4)$$

where X_i stands for the yearly rainfall for the period under study; \bar{X} represents the long-term average yearly rainfall for the observation period and σ corresponds to the standard deviation of yearly rainfall during the observed period (Alemu & Bawoke 2019). Table 3 shows the SAI value classification used.

Mann-Kendall trend test, Sen's slope estimator and projected changes

The study employed the Mann-Kendall (MK) trend statistics to assess trends in rainfall, and Sen's slope estimator was also used to determine the magnitude of the trends over the ORB. The MAKESENS Software was used to compute the trends at a 5% significance level. The test is universally acknowledged due to its robustness, least susceptible to outliers and appropriate for discovering tendencies in time series records (Siraj *et al.* 2013). It is the most commonly recommended test, and it has

Table 3 | SAI value classification (McKee *et al.* 1993)

SAI value	Category
Above 2	Extremely wet
1.5 to 1.99	Very wet
1.0 to 1.49	Moderately wet
−0.99 to 0.99	Near normal
−1.0 to −1.49	Moderately dry
−1.5 to −1.99	Severely dry
−2 or less	Extremely dry

been used in a number of research to assess trends in rainfall (Yue *et al.* 2002; Seleshi & Zanke 2004; Kiros *et al.* 2016). The MK test compares the null hypothesis (H_0) of no trend to the alternative hypothesis (H_1) that there is a trend (Önöz & Bayazit 2003). Positive values of the MK test show rising trends, whereas negative values indicate declining trends. Sen's slope (β) estimation test computes the gradient (i.e., the linear rate of change), and it is a linear regression test. A positive value of β demonstrates an 'upward trend' or an increase, while a negative value shows a 'downward trend' or a decrease. No change is represented by a Zero β (Ayanlade *et al.* 2018). The rainfall change is the difference in yearly average rainfall between the observed (1981–2010) and future periods (2021–2050).

RESULTS AND DISCUSSION

RCMs' performance and bias-correction

The result obtained for comparing the RCMs with the observation is demonstrated on the Taylor diagram in Figure 2. It can be seen that the correlation values obtained from the comparison are above 0.9, with a standard deviation value below 2.0 and an RMSE value below 0.75. The CNRM-CM5 model had the strongest correlation ($R=0.99$), the least centered RMSE (below 0.25) and a lowest standard deviation (below 1.25). Although the GFDL-ESM2M model was found to be the weakest, it recorded a correlation of 0.93, a centered RMSE below 0.75 and a standard deviation below 1.75. Although the CNRM-CM5 model performed best among the individual models, the models' ensemble also performed better than most single models with a correlation of 0.98, RMSE below 0.25 and standard deviation below 1.25. The findings are similar to those of Akinsanola *et al.* (2017) and Lin *et al.* (2020), who also noted that models' ensemble mean makes the representation of rainfall characteristics better than the majority of single models. Generally, the results show a close match between the RCMs and ensemble simulated rainfall pattern and observation.

Figure 3 provides the result from the bias-correction of the eight CORDEX-Africa RCMs. The correlation between the raw models' ensemble and observation were 0.76 and the NSE value of 0.53. The uncorrected models each show clear variances in how it reproduces historical rainfall (Figure 3(a)). However, after bias-correction, the individual models and their ensemble are seen to be enhanced (Figure 3(b)). After bias-correction, a correlation between the ensemble and observed was 0.91 with an improved NSE (0.98). Generally, it is observed that the corrected individual RCMs and their ensemble were improved to reproduce the rainfall pattern demonstrated by the observed records at the monthly scale. Hence, the bias-corrected RCMs can be said to represent the ORB and are considered reliable for the analysis.

Month-to-month distribution of rainfall

Figure 4 illustrates the annual cycle of rainfall per month for both observed (1981–2010) and near-future periods (2021–2050) under RCP4.5 and RCP8.5. It is observed that the monthly rainfall for the future period would have its peak in August just like the observed period. The amount of rainfall for the peak season, August, is revealed to be 246.1 mm for the observed period; 246.8 mm (about 0.26% peak increment) and 269 mm (about 9.3% increment) of rainfall in the near-future period for RCP4.5 and RCP8.5, respectively. The expected rise in rainfall during the peak month could cause the basin to experience some flooding episodes, and great disturbance to agricultural production (crops and livestock). It can also lead to the outbreak of rain-related diseases like malaria. It is worthy to note that the basin's adaptation and mitigation efforts be strengthened during this period so as to help curb the occurrence of any devastating situations.

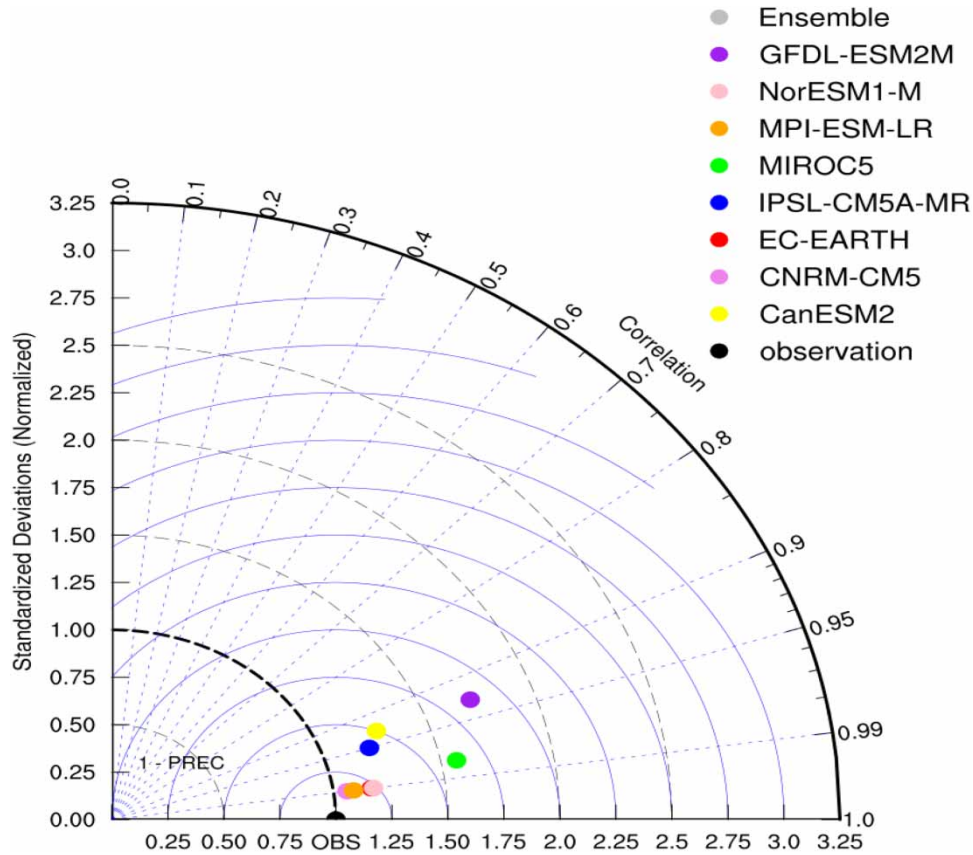


Figure 2 | Taylor diagram displaying RCMs' efficiency based on standardized deviation (normalized), correlation and centered root-mean-square error between the simulated and observed patterns of monthly mean rainfall across the ORB.

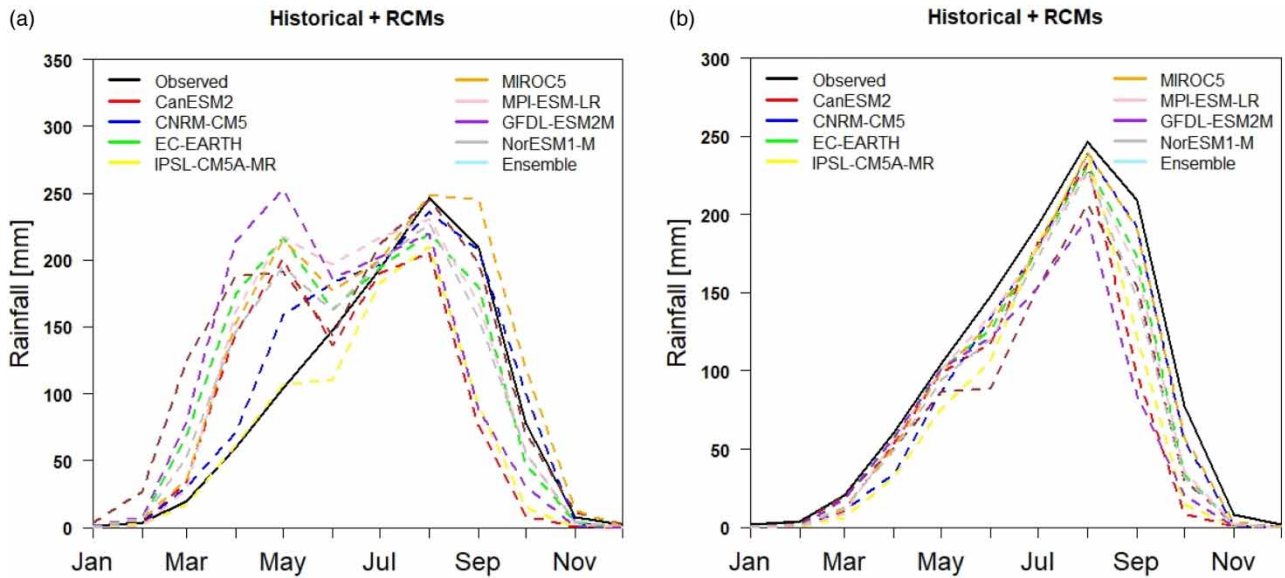


Figure 3 | Comparison of observed and simulated rainfall at a monthly scale: (a) uncorrected and (b) bias-corrected.

The amount of rainfall for the rainy season (April–October) (Klassou & Komi 2021) is expected to be around 947.7 mm (a decrease of about 8.8%) under the RCP4.5 scenario and around 1,004 mm (3.4% decrease in rainfall amount) for the RCP8.5 scenario comparing with the observed, which recorded 1,038.8 mm of rainfall. For the dry season (November–March), the

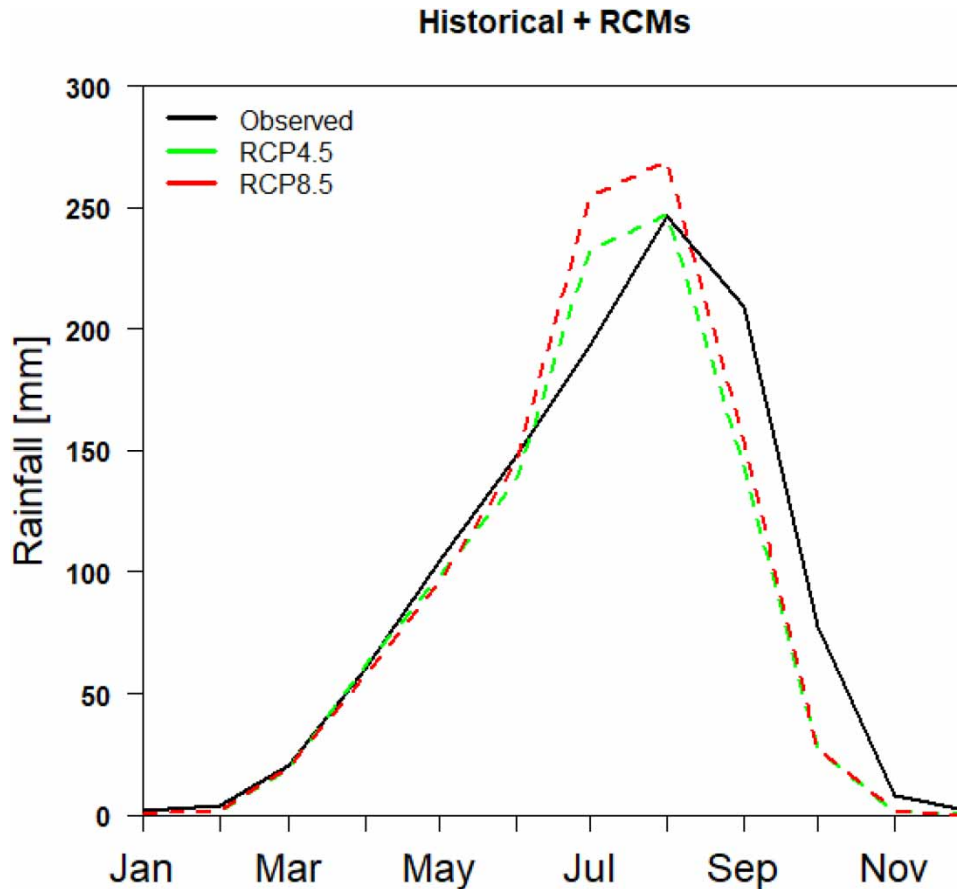


Figure 4 | Annual cycle of monthly rainfall for the observed period 1981–2010 (black line) and future rainfall projections for 2021–2050 for the RCP4.5 scenario (green-dashed line) and the RCP8.5 scenario (red-dashed line). Please refer to the online version of this paper to see this figure in color: <http://dx.doi.org/10.2166/wcc.2022.368>.

amount of rainfall is expected to be around 22.5 mm (a decrease of about 36.4%) under RCP4.5 and about 24 mm (a decrease of about 32.3%) for the RCP8.5 scenario in relation to the observed rainfall of 35.4 mm. As water is crucial to crop production in the basin and agriculture in the region being highly rainfall-dependent, the projections of future rainfall change could greatly influence crop production (Reilly *et al.* 2003; Olesen *et al.* 2007; Gornall *et al.* 2010).

Annual rainfall distribution

Mean, standard deviation (SD) and CV were computed for 1981–2010 and 2021–2050 (Table 4). During the observed period, mean annual rainfall was 1,073.9 mm which ranged between 783.4 mm at GRID3 and 1,464.8 mm at GRID20. The mean annual rainfall during the 2021–2050 period recorded 970.2 mm under RCP4.5, which ranged between 640.2 mm at GRID3 and 1,408.3 mm at Sokode; and 1,027.9 mm under the RCP8.5 scenario, which also ranged from 758.4 mm at GRID3 to 1,287.1 mm at Sokode. It is observed that the lower basin receives a high amount of rainfall as compared to the middle and upper basins during the observed and future periods. Although rainfall in the lower basin would rise in the future period, the amount would be reduced. The study discovered a reduction in the mean annual rainfall for the future period under both emission scenarios. This could reflect the predictions of the IPCC (2007) that subtropical areas would experience a decreased rainfall due to the changing climate.

Figure 5 illustrates the allocation of rainfall spatially at the basin for observed and future periods. It is generally seen that rainfall in the basin is more pronounced in the lower basin as compared to the upper basin. Rainfall would generally decrease entirely across the basin under the RCP4.5 scenario. However, under RCP8.5, rainfall in the lower basin would further decrease, while the upper basin would experience a slight recovery of rainfall. Similarly, rainfall is expected to decline in future under both climate scenarios at a temporal scale (Figure 6). From the time series, it is detected that annual rainfall in the basin during the historical period was between 835.5 mm (1983) and 1,239.1 mm (2009). In the future period and

Table 4 | Summary statistics of rainfall in the ORB

Station	Observed (1981–2010)			RCP4.5 (2021–2050)			RCP8.5 (2021–2050)		
	Mean (mm)	SD (mm)	CV (%)	Mean (mm)	SD (mm)	CV (%)	Mean (mm)	SD (mm)	CV (%)
GRID1	792.9	94.8	12.0	684.1	59.6	8.7	834.3	65.8	7.9
GRID2	815.6	115.6	14.2	693.4	63.3	9.1	839.2	55.4	6.6
GRID3	783.4	120.4	15.4	640.2	62.0	9.7	758.4	54.5	7.2
GRID4	853.6	130.4	15.3	712.7	62.9	8.8	835.9	64.7	7.7
GRID5	891.6	110.5	12.4	774.7	65.0	8.4	922.0	76.9	8.3
GRID6	877.2	107.2	12.2	773.1	62.0	8.0	896.1	76.0	8.5
GRID7	886.0	134.1	15.1	792.0	58.5	7.4	898.7	74.7	8.3
GRID8	928.6	137.5	14.8	829.3	69.2	8.3	915.9	68.5	7.5
GRID9	974.9	129.5	13.3	866.8	64.2	7.4	927.5	63.3	6.8
GRID10	941.8	113.3	12.0	885.7	63.9	7.2	1,006.3	74.6	7.4
GRID11	943.7	126.4	13.4	872.7	60.8	7.0	957.5	63.7	6.7
GRID12	1,074.7	141.2	13.1	932.1	70.8	7.6	1,006.6	70.8	7.0
GRID13	982.5	107.9	11.0	845.9	61.8	7.3	914.2	69.8	7.6
GRID14	1,101.5	112.2	10.2	1,038.0	70.2	6.8	1,117.4	64.4	5.8
GRID15	1,200.3	132.5	11.0	1,108.6	62.8	5.7	1,124.9	60.7	5.4
GRID16	1,239.3	126.6	10.2	1,174.1	81.9	7.0	1,193.7	59.5	5.0
GRID17	1,330.6	170.1	12.8	1,279.0	95.0	7.4	1,266.1	72.4	5.7
GRID18	1,363.5	163.8	12.0	1,164.4	88.6	7.6	1,128.0	70.4	6.2
GRID19	1,360.3	194.4	14.3	1,295.4	69.5	5.4	1,227.5	73.3	6.0
GRID20	1,464.8	207.2	14.1	1,293.5	90.3	7.0	1,212.1	77.9	6.4
Natitingou	1,187.5	174.5	14.7	1,045.2	64.9	6.2	1,091.7	87.8	8.0
Fada	819.4	137.8	16.8	688.9	65.2	9.5	852.2	76.9	9.0
Tenkodogo	819.0	119.0	14.5	740.3	56.4	7.6	887.4	78.4	8.8
Kete-Krachi	1,358.6	320.9	23.6	1,332.6	94.3	7.1	1,249.1	91.2	7.3
Yendi	1,210.1	217.4	18.0	1,153.2	81.6	7.1	1,148.2	71.4	6.2
Dapaong	1,061.5	215.2	20.3	894.7	63.2	7.1	1,012.5	80.3	7.9
Kara	1,289.1	195.3	15.1	1,134.2	81.1	7.1	1,149.0	83.6	7.3
Mango	1,045.2	157.0	15.0	986.1	66.4	6.7	1,096.5	67.5	6.2
Niamtougou	1,361.9	200.3	14.7	1,067.7	78.9	7.4	1,082.2	77.3	7.1
Sokode	1,266.8	171.3	13.5	1,408.3	100.9	7.2	1,287.1	73.3	5.7
Basin	1,073.8	104.1	9.7	970.2	52.8	5.4	1,027.9	51.4	5.0

SD, standard deviation; CV, coefficient of variation.

under RCP4.5, annual rainfall is expected to range between 842.4 mm (2027) and 1,082.3 mm (2037); and between 900.6 mm (2041) and 1,126.1 mm (2028) of rainfall for RCP8.5. Declined rainfall anticipated at both spatial and temporal scales could severely impact agricultural planning and crop production in the basin. In addition, it could greatly impact streamflow and water levels in the basin. Subsequently, the existing adaptation strategies in the basin must be evaluated in order to ensure that the livelihoods of peripheral communities are not hindered by expected changes.

Projections in annual rainfall

Figure 7 and Table 5 show the projected changes in rainfall at the ORB. For RCP4.5, almost all stations would experience a reduced amount of rainfall except for the Sokode station which recorded an increment. Similarly, under RCP8.5 in the future, the majority of the stations in the basin would experience a reduced amount of rainfall (particularly stations in the lower

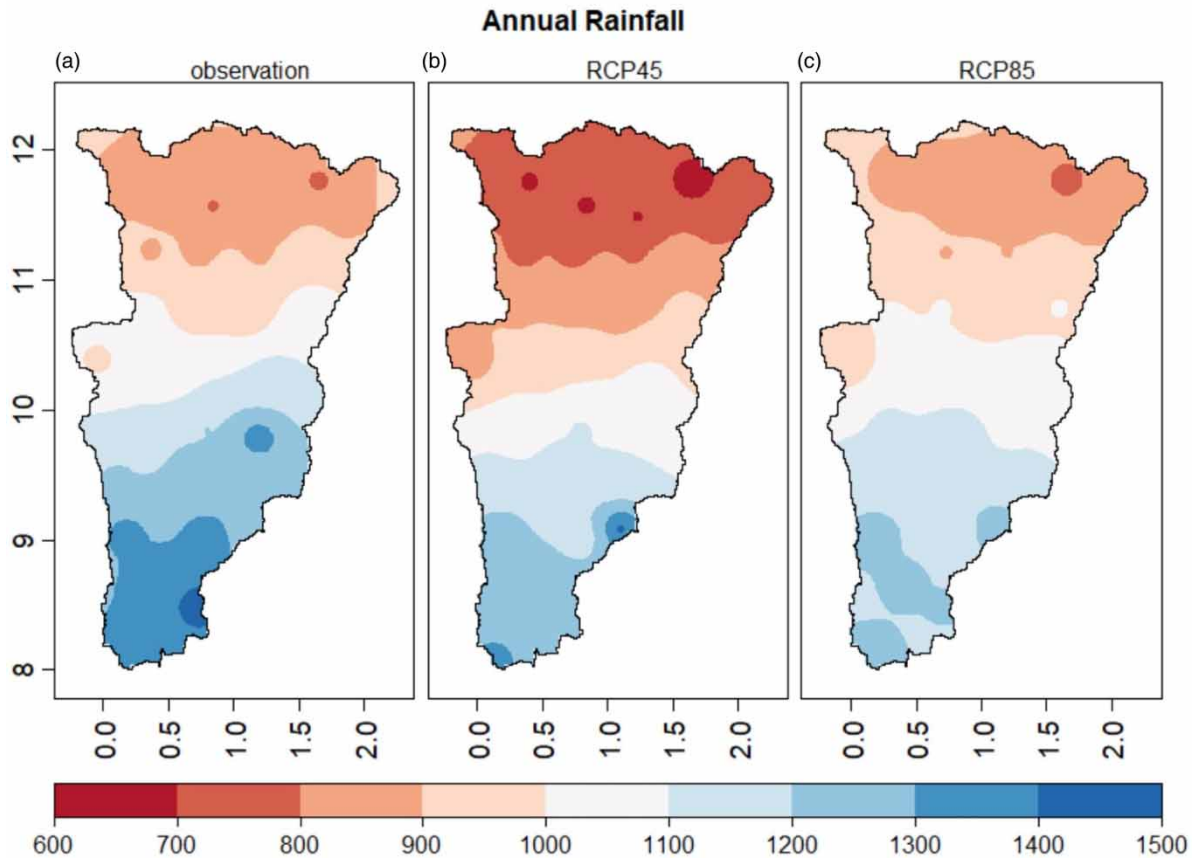


Figure 5 | Spatial distribution of annual rainfall (mm) for (a) the observed period (1981–2010), (b) the future period (2021–2050) under the RCP4.5 scenario and (c) the future period (2021–2050) under the RCP8.5 scenario at the ORB.

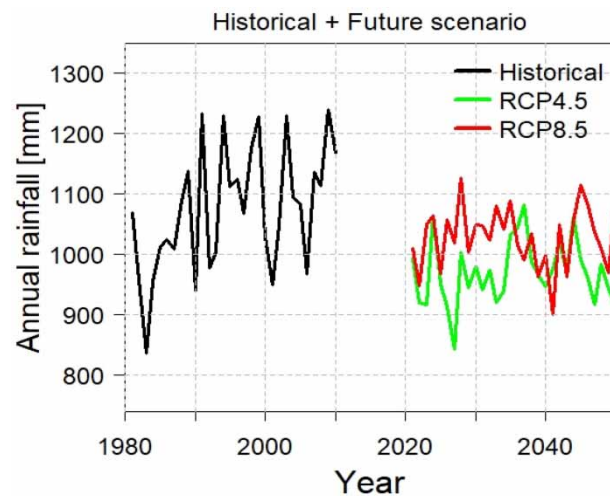


Figure 6 | Temporal distribution of annual rainfall (mm). The annual rainfall for the historical period (1981–2010) is shown in black, while the future period (2021–2050) trends are shown in green and red for RCP4.5 and RCP8.5 emission scenarios, respectively.

basin), except for a few stations which would record an increment in rainfall. Rainfed agriculture in the West African sub-region could significantly be at risk (Owusu & Waylen 2009). In addition, Lare & Nicholson (1994) have pointed out that inadequate large-scale rainfall, as shown at the stations, can affect ecosystems. The MK test for annual rainfall in the basin

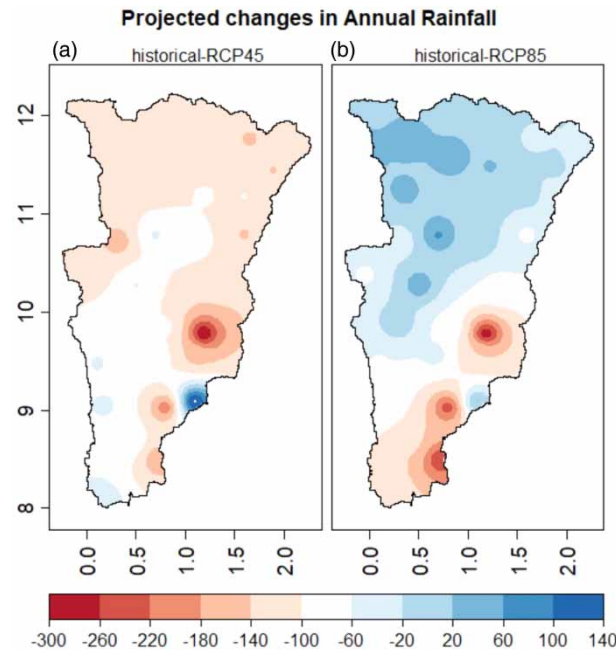


Figure 7 | Projected changes in annual rainfall (mm) (a) under RCP4.5 and (b) RCP8.5 scenarios at the ORB for 2021–2050 relative to the historical period (1981–2010).

revealed a significant increasing trend as well as stations such as GRID1–GRID12, GRID 15, Natitingou and Dapaong for the observed period (1981–2010). The MK test for the basin during the future period (2021–2050) under RCP4.5 exposed an insignificant increasing trend at a 5% significant level. However, the Niamtougou station revealed a significant increasing trend. Rainfall across the basin revealed an insignificant decreasing trend in the future (2021–2050) for the RCP8.5 scenario (Table 6).

Variability of rainfall for observed (1981–2010) and future periods (2021–2050)

The standard deviation ranged between 94.8 mm at GRID1 and 320.9 mm of rainfall at Kete-Krachi with a mean value of 104.1 mm. CV varied from 10.2% at GRID16 to 23.6% at Kete-Krachi with a mean CV of 9.7%, indicating less rainfall variability (<20%) according to *Asfaw et al. (2018)* and *Alemu & Bawoke (2019)*. The moderate variability in rainfall at Kete-Krachi (23.6%) and Dapaong (20.3%) suggests that the amount of water available in these areas was somewhat more erratic compared to the areas with low CV (*Alemu & Bawoke 2019*).

The mean standard deviation recorded under RCP4.5 was 52.8 mm for the basin, which varied from 56.4 mm at Fada to 100.9 mm at Niamtougou. Under the RCP8.5, the mean standard deviation is 51.4 mm for the basin, ranging between 54.5 mm at GRID3 and 91.2 mm at Sokode. The mean CV in the basin recorded for RCP4.5 was 5.4% ranging from 5.4% at GRID19 to 9.7% at GRID3. The mean CV in the basin under the RCP8.5 scenario recorded 5% which ranged between 5% at GRID16 and 9% at Natitingou. This shows a low variation of rainfall for RCP4.5 and RCP8.5 scenarios. Although almost all stations revealed a low to moderate variation in rainfall amount for the understudied periods, studies such as *Nyatume & Agodzo (2017)*, *Ayanlade et al. (2018)* and *Alemu & Bawoke (2019)* have stated that such variations can adversely impact agriculture and water management. The spatial distribution of CV for annual rainfall is given in Figure 8. The CV for the entire basin was found to be high during the historical period but shows a general increase from the lower basin to the upper basin.

Anomalies of rainfall for observed (1981–2010) and future periods (2021–2050)

The annual rainfall anomalies in the ORB for the observed (1981–2010) and future periods (2021–2050) under RCPs 4.5 and 8.5 scenarios are shown in Figures 9 and 10, respectively. The results exposed the year-to-year variations in rainfall across the basin. The year 2009 is seen to have had the highest positive anomaly (+1.58), while 1983 had the highest negative anomaly (−2.29). This conforms with the study by *Kasei et al. (2010)*, which found out that 1983 was the driest year in the Volta Basin.

Table 5 | Projection of mean annual rainfall at the ORB (2021–2050)

Stations	Mean annual rainfall and change (mm)				
	(1981–2010)		Future (2021–2050)		
	Observed	RCP4.5	Change	RCP8.5	Change
GRID1	792.9	684.2	−108.7	834.3	41.4
GRID2	815.6	693.4	−122.2	839.2	23.6
GRID3	783.4	640.2	−143.2	758.4	−25.0
GRID4	853.6	712.7	−141.0	835.9	−17.7
GRID5	891.6	774.7	−116.8	922.0	30.5
GRID6	877.2	773.1	−104.1	896.1	18.9
GRID7	886.0	792.0	−94.0	898.7	12.7
GRID8	928.6	829.3	−99.3	915.9	−12.7
GRID9	974.9	866.8	−108.2	927.5	−47.4
GRID10	941.8	885.8	−56.0	1,006.3	64.5
GRID11	943.7	872.7	−71.1	957.5	13.8
GRID12	1,074.7	932.2	−142.6	1,006.6	−68.1
GRID13	982.5	845.9	−136.6	914.2	−68.3
GRID14	1,101.5	1,038.0	−63.4	1,117.4	16.0
GRID15	1,200.3	1,108.6	−91.7	1,124.9	−75.3
GRID16	1,239.3	1,174.1	−65.2	1,193.7	−45.7
GRID17	1,330.6	1,279.0	−51.6	1,266.1	−64.5
GRID18	1,363.5	1,164.4	−199.1	1,128.0	−235.5
GRID19	1,360.3	1,295.4	−64.9	1,227.5	−132.9
GRID20	1,464.8	1,293.5	−171.3	1,212.1	−252.7
Natitingou	1,187.5	1,045.2	−142.3	1,091.7	−95.7
Fada	819.4	688.9	−130.5	852.2	32.8
Tenkodogo	819.0	740.3	−78.7	887.4	68.4
Kete-Krachi	1,358.6	1,332.6	−26.0	1,249.1	−109.5
Yendi	1,210.1	1,153.2	−56.9	1,148.2	−61.9
Dapaong	1,061.5	894.7	−166.8	1,012.5	−49.0
Kara	1,289.1	1,134.2	−154.9	1,149.0	−140.0
Mango	1,045.2	986.1	−59.1	1,096.5	51.3
Niamtougou	1,361.9	1,067.7	−294.2	1,082.3	−279.6
Sokode	1,266.8	1,408.3	141.5	1,287.1	20.3
Basin	1,073.8	970.2	−103.6	1,027.9	−45.9

More than 90% of the basin was in a severe state of drought and a moderate drought occurred prior to 1982. From the results, the early 1980s experienced pronounced negative anomalies. This shows a relationship with the historic drought in the basin and West Africa between 1961 and 2005 (Kasei *et al.* 2010). This resulted in the loss of lives and farm animals in desertlike areas of Burkina Faso (Dembélé & Zwart 2016). Generally, the historical period had 4 very wet years (1991, 1994, 2003 and 2009), 1 moderately wet year (1999), 5 moderately dry years (1982, 1984, 1990, 2001 and 2006), 1 extremely dry year (1983) and the remaining 19 years being near normal years. The SAI for the future period is displayed in Figure 10. In the future period, the negative anomaly would be more pronounced in 2027 (−2.42) under RCP4.5 and in 2041 (−2.48) under the RCP8.5 scenario, indicating a possibility of extremely dry conditions. The positive anomaly is expected to be more pronounced in 2037 (2.12) under RCP4.5 and 2028 (1.91) under RCP8.5, indicating extremely wet and very wet periods,

Table 6 | MK trend test and Sen's slope estimates

Station	Observed (1981–2010)		RCP4.5 (2021–2050)		RCP8.5 (2021–2050)	
	Z value	S. slope	Z value	S. slope	Z value	S. slope
GRID1	2.36	4.69	1.25	1.61	-1.21	-1.83
GRID2	2.71	5.28	1.28	1.81	-0.68	-0.79
GRID3	2.82	5.15	0.50	0.75	-0.64	-0.69
GRID4	2.32	4.98	0.57	1.20	-0.14	-0.32
GRID5	2.53	6.36	1.11	1.84	-1.32	-2.76
GRID6	2.6	6.14	1.61	1.71	-0.46	-0.93
GRID7	3.03	6.67	0.86	1.26	-0.71	-0.78
GRID8	2.96	7.69	0.61	0.99	0.64	1.33
GRID9	3.00	7.09	0.07	0.28	1.25	1.35
GRID10	2.68	6.63	0.25	0.63	0.43	0.58
GRID11	3.28	7.96	0.43	0.58	0.61	0.72
GRID12	3.28	8.7	1.00	1.63	1.03	2.25
GRID13	1.21	3.06	0.36	0.66	0.07	0.10
GRID14	1.25	3.38	0.14	0.16	1.25	1.59
GRID15	2.11	6.17	0.71	0.64	1.00	1.59
GRID16	1.89	5.87	-0.39	-0.93	0.82	1.22
GRID17	0.82	2.67	0.07	0.07	0.29	0.33
GRID18	1.57	4.82	1.46	3.18	1.18	2.21
GRID19	0.75	4.08	-0.25	-0.52	0.21	0.18
GRID20	1.75	7.37	0.86	2.22	1.57	2.81
Natitingou	1.86	6.69	1.03	2.01	0.57	1.16
Fada	2.28	8.2	1.50	2.71	-0.93	-1.48
Tenkodogo	1.57	3.83	0.50	0.55	-1.53	-2.06
Kete-Krachi	0.82	4.93	-1.36	-2.70	-0.11	-0.43
Yendi	1.89	9.88	-0.86	-1.67	1.25	1.91
Dapaong	2.68	11.63	-0.11	-0.10	-0.96	-1.63
Kara	1.00	3.38	1.89	3.36	0.07	0.29
Mango	-0.5	-0.94	-0.04	-0.10	0.50	0.93
Niamtougou	1.75	7.77	2.07	3.35	0.14	0.33
Sokode	1.12	4.73	0.36	0.62	0.18	0.25
Basin	2.50	5.84	0.43	0.58	-0.04	-0.05

Note: values in bold are significant at 5%; S. slope=Sen's slope.

respectively (McKee *et al.* 1993). Thus, the RCP4.5 scenario would experience 1 extremely wet year (2037), 2 very wet years (2024 and 2044), 2 moderately wet years (2035 and 2036), 3 moderately dry years (2023, 2026 and 2047), 1 extremely dry year (2027) and the rest of the 21 years experiencing near normal years. The RCP8.5 scenario would experience 2 very wet years (2028 and 2045), 3 moderately wet years (2033, 2035 and 2046), 4 moderately dry years (2025, 2039, 2043 and 2049), 1 severely dry year (2022), 1 extremely dry year (2041) and the remaining 19 years experiencing near normal years. The predicted very wet and extremely wet years could lead to flood incidences, which could have impacts on human lives and property (Klassou & Komi 2021). Water scarcity in the basin could occur from the basin's moderately dry, severely dry and extremely dry years. Long dry seasons caused by climate change result in water scarcity, harming people's health and crop productivity (Zhang *et al.* 2015).

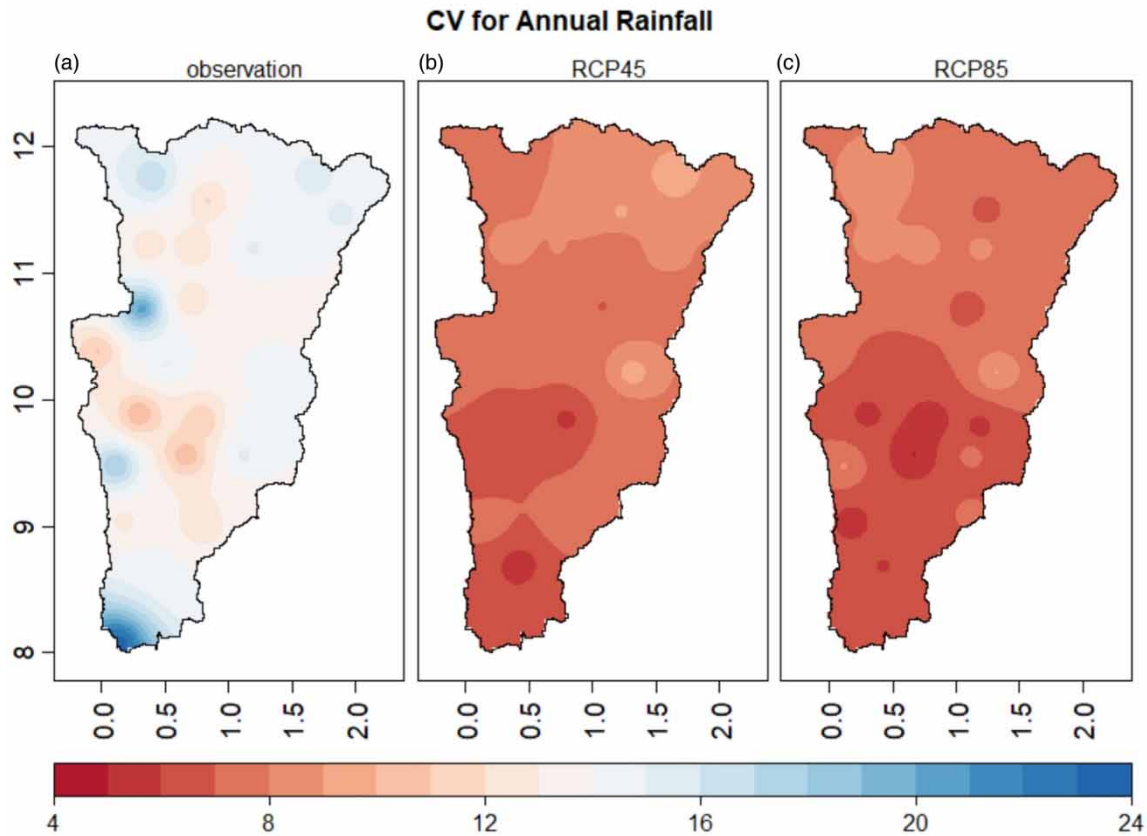


Figure 8 | Spatial distribution of CV (%) for (a) the observed period (1981–2010), (b) the future period (2021–2050) under the RCP4.5 scenario and (c) the future period (2021–2050) under the RCP8.5 scenario in the ORB.

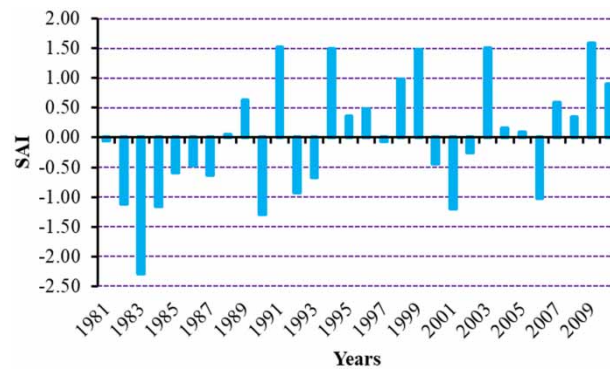


Figure 9 | Annual rainfall anomalies of the ORB for the observed period (1981–2010).

Implications of projected variation in rainfall on land use and water yield

Cropland is seen to be the dominant land use in the ORB from the 2016 land-use land-cover map (Figure 11). Farming covers areas from latitude 9°N to the northern part of the basin, which was observed to have an annual rainfall between 800 and 1,300 mm (Figure 5). The projected changes under RCP4.5 (decrease between 20 and 180 mm) could make the forest areas below latitude 9°N also suitable climatologically for farming if soil and other factors are conducive (Travis 2016). Moreover, the projected decrease in the upper basin may influence a shift or gradual migration of cropping areas toward the lower basin. On the other hand, the projected increase in annual rainfall under RCP8.5 from the middle basin toward the upper

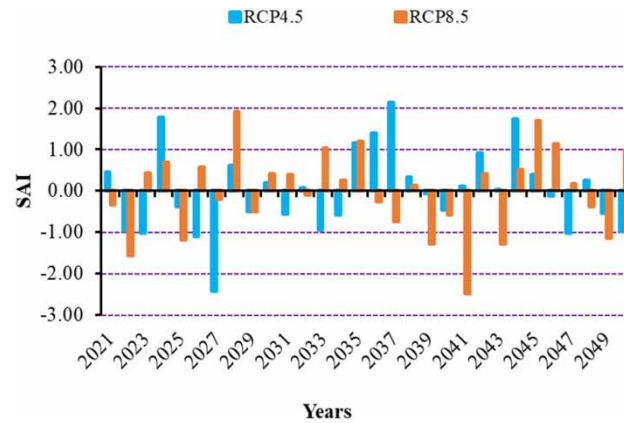


Figure 10 | Annual rainfall anomalies of the ORB for the future period (2021–2050) under RCP4.5 and RCP8.5 scenarios.

basin could result in changes of cropping systems that make use of the additional rainfall amount (Chemura *et al.* 2020). Also, it might imply that more water-resilient varieties would be needed. Grassland and cropland may be expanded to meet up with demands of food and livestock feed as climate change adaptation or coping strategies in the ORB. This means that as an exchange for higher agricultural productivity in the basin, the conversions to cropland can affect the ecosystem services predominantly, especially water yield due to increased runoff (Brink & Eva 2009; Li *et al.* 2018). Changes in land use, particularly the continuous expansion of cropland, have contributed to the degradation of vegetation and water scarcity in recent years, as reported elsewhere (Sajikumar & Remya 2015; Woldesenbet *et al.* 2017; Balist *et al.* 2022). Land-use/land-cover changes alter the rainfall path into runoff by affecting important hydrological elements like surface runoff, groundwater recharge, infiltration, interception and evaporation (Song & Deng 2017; Woldesenbet *et al.* 2017; Balist *et al.* 2022). Water yield is one of the most important ecosystem services, and it is critical to the regional economy and ecosystem's long-term sustainability (Yang *et al.* 2021). The spatial distribution of CV of rainfall in the basin (Figure 8) shows that extreme changes may not occur and, therefore, could prevent sudden migration of farm activities from one location to the other. As the ORB is also crucial to the West African sub-region's economy, it is obvious that the expansion of cropland and decline in tree cover may become vital environmental stressors and subsequently impact surface runoff and water yield in the basin. In addition, the anticipated decline in rainfall in the basin during the near-future period (2021–2050) under both RCP4.5 and RCP8.5 scenarios calls for an evaluation of land use and climate impacts on water yield in the basin in order to know the future water availability.

CONCLUSIONS

This work has investigated rainfall variations and anticipated change over the ORB for observed (1981–2010) and future periods (2021–2050) under RCP4.5 and RCP8.5, using data from meteorological stations, CHIRPS gridded-observed data as well as CORDEX-Africa. Percentage change in rainfall for the peak month as well as for rainy and dry seasons under the two climate scenarios was determined at a monthly scale. The mean annual rainfall in the ORB was 1,073.9 mm, SD of 104.1 mm and CV of 9.7% for the observed period. The annual average rain in the future period under RCP4.5 recorded 970.2 mm, SD of 52.8 mm and CV of 5.4%. Under RCP8.5, the basin recorded 1,027.9 mm average rainfall which had SD and CV of 51.4 mm and 5%, respectively. Generally, rainfall amount would decline under both emission scenarios. At a monthly scale, percentage rainfall increment for the peak month (August) is expected to be around 0.26% for RCP4.5 and 9.3% under RCP8.5. The amount of rainfall for the rainy (April–October) and dry seasons (November–March) would experience a decrease under both climate scenarios. Also, during the observed period, the highest positive anomaly of 1.58 was seen in 2009, with the highest negative anomaly (−2.29) recorded in 1983 revealing a connection with historic drought conditions. The year 2037 would experience a more positive anomaly (2.12), while a high negative anomaly (−2.42) is expected to be recorded in 2027 under RCP4.5 disclosing a possible very wet and extremely dry situation. Also, a high positive anomaly in the year 2028 (1.91) and a high negative anomaly (−2.48) in the year 2041 under RCP8.5 are observed, unveiling a very wet and extremely dry condition to be expected, respectively. The trend analysis presented both statistically nonsignificant growing and declining movement for RCP4.5 and RCP8.5, respectively, with the historical period revealing a significant

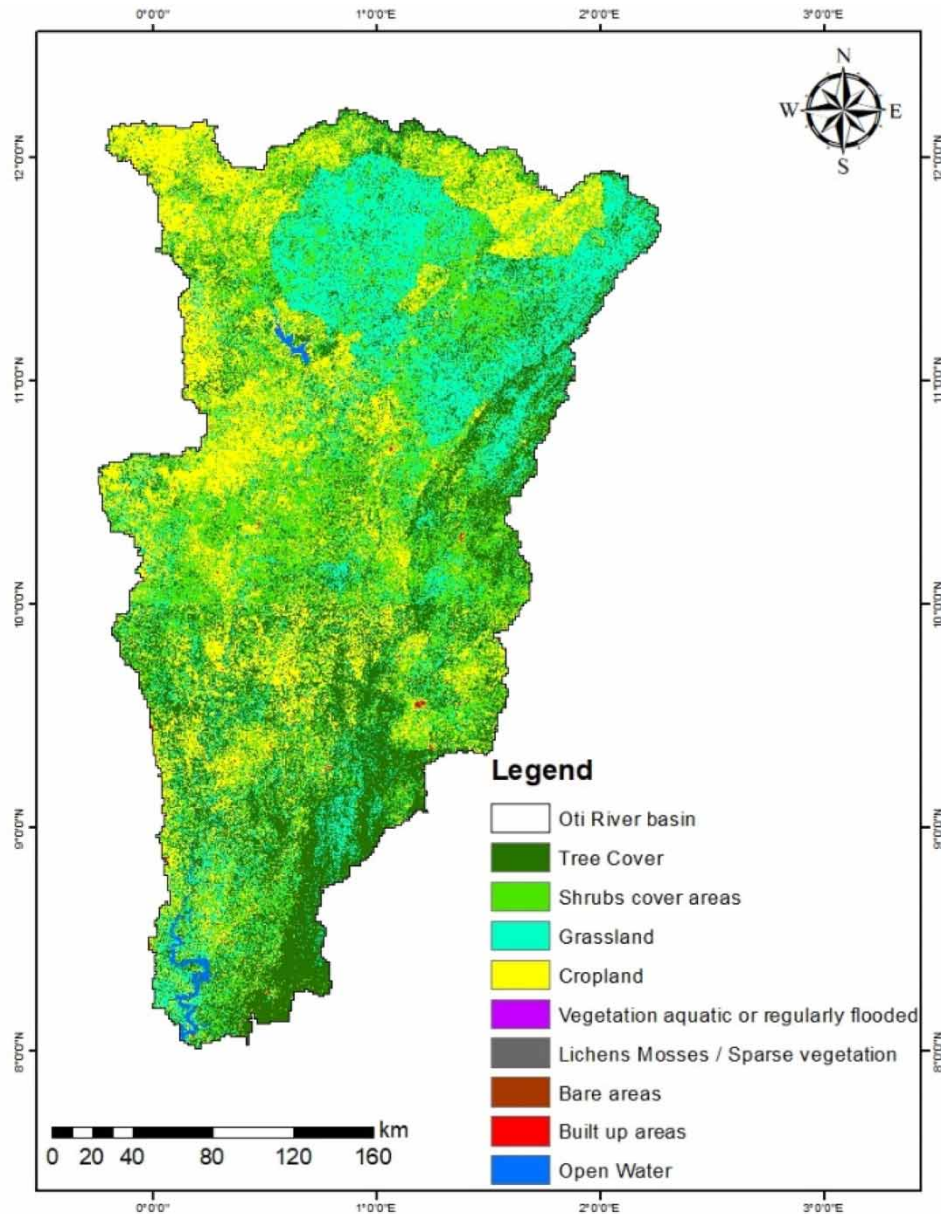


Figure 11 | Sentinel-2 (S2) 2016 prototype land-cover map of the ORB from the 20 m Africa land-cover map by the European Space Agency (ESA).

increasing trend. The expected decrease in rainfall is cause for concern because it signifies that the dependent countries' source of livelihood and economic boost could be endangered. In addition, the expected moderately dry, severely dry and extremely dry years in the future could throw off the balance between water demand and availability, putting basin-dependent countries in a water stress situation. Although the study relied on gridded datasets to complement missing data, its finding offers crucial information for a better understanding of the spatiotemporal distribution and variations necessary for the sustenance of economic development and livelihoods through such sectors as agriculture, water resources, ecosystem and biodiversity. However, the impact of projections on land use and water yield could only be inferred. Therefore, modeling the basin hydrology for the accessibility of water in the future is advised. Research would be necessary to assess the impacts of land-use and land-cover changes on rainfall variability and change over the basin. Additionally, the future study should concentrate on climate change resilient management strategies in the ORB.

ACKNOWLEDGEMENTS

The German Federal Ministry of Education and Research (BMBF) via the West African Science Service Center on Climate Change and Adapted Land Use (WASCAL) supported this work, which is a section of the first authors' Doctoral study at Université d'Abomey-Calavi, Benin. The authors acknowledge the national meteorological agencies of Ghana, Togo and Benin for the rainfall data, and also CHIRPS and the CORDEX-Africa project for making their data accessible.

CONFLICT OF INTEREST

The authors declare no conflict of interest.

DATA AVAILABILITY STATEMENT

Data cannot be made publicly available; readers should contact the corresponding author for details.

REFERENCES

- Aguilar, E., Barry, A. A., Brunet, M., Ekang, L., Fernandes, A., Massoukina, M., Mbah, J., Mhanda, A., do Nascimento, D. J., Peterson, T. C., Uamba, O. T., Tomou, M. & Zhang, X. 2009 *Changes in temperature and precipitation extremes in western central Africa, Guinea Conakry, and Zimbabwe, 1955–2006*. *Journal of Geophysical Research Atmospheres* **114** (2), 1–11. <https://doi.org/10.1029/2008JD011010>.
- Agyekum, J., Annor, T., Lamptey, B., Quansah, E. & Agyeman, R. Y. K. 2018 *Evaluation of CMIP5 global climate models over the Volta Basin: precipitation*. *Advances in Meteorology* **2018**, 4853681. <https://doi.org/10.1155/2018/4853681>.
- Akinsanola, A. A., Ajayi, V. O., Adejare, A. T., Adeyeri, O. E., Gbode, I. E., Ogunjobi, K. O., Nikulin, G. & Abolude, A. T. 2017 *Evaluation of rainfall simulations over West Africa in dynamically downscaled CMIP5 global circulation models*. *Theoretical and Applied Climatology* **132** (1–2), 437–450. <https://doi.org/10.1007/s00704-017-2087-8>.
- Akumaga, U. & Tarhule, A. 2018 *Projected changes in intra-season rainfall characteristics in the Niger River Basin, West Africa*. *Atmosphere* **9** (12), 1983–1985. <https://doi.org/10.3390/atmos9120497>.
- Alemu, M. M. & Bawoke, G. T. 2019 *Analysis of spatial variability and temporal trends of rainfall in Amhara Region, Ethiopia*. *Journal of Water and Climate Change* **11** (4), 1505–1520. <https://doi.org/10.2166/wcc.2019.084>.
- Ampadu, B. 2021 *Overview of hydrological and climatic studies in Africa: the case of Ghana*. *Cogent Engineering* **8** (1), 1914288. <https://doi.org/10.1080/23311916.2021.1914288>.
- Annor, T., Lamptey, B., Wagner, S., Oguntunde, P., Arnault, J., Heinzeller, D. & Kunstmann, H. 2017 *High-resolution long-term WRF climate simulations over Volta Basin. Part 1: validation analysis for temperature and precipitation*. *Theoretical and Applied Climatology* **133**, 829–849. <https://doi.org/10.1007/s00704-017-2223-5>.
- Asfaw, A., Simane, B., Hassen, A. & Bantider, A. 2018 *Variability and time series trend analysis of rainfall and temperature in northcentral Ethiopia: a case study in Woleka sub-basin*. *Weather and Climate Extremes* **19**, 29–41. <https://doi.org/10.1016/j.wace.2017.12.002>.
- Ayanlade, A., Radeny, M., Morton, J. F. & Muchaba, T. 2018 *Rainfall variability and drought characteristics in two agro-climatic zones: an assessment of climate change challenges in Africa*. *Science of the Total Environment* **630**, 728–737. <https://doi.org/10.1016/j.scitotenv.2018.02.196>.
- Badjana, H. M., Selsam, P., Wala, K., Flügel, W.-A., Fink, M., Urban, M., Helmschrot, J., Afouda, A. & Akpagana, K. 2014 *Assessment of land-cover dynamics in a sub-catchment of Oti basin (West Africa): a case study of Kara river basin*. *Zentralblatt für Geologie und Paläontologie, Teil I* **1**, 151–170. <https://doi.org/10.1127/zgpI/2014/0151-0170>.
- Balist, J., Malekmohammadi, B., Jafari, H. R., Nohegar, A. & Geneletti, D. 2022 *Detecting land use and climate impacts on water yield ecosystem service in arid and semi-arid areas. A study in Sirvan River Basin-Iran*. *Applied Water Science* **12** (1), 1–14. <https://doi.org/10.1007/s13201-021-01545-8>.
- Barry, B., Obuobie, E., Andreini, M., Andah, W. & Pluquet, M. 2005 *The Volta River Basin. Comprehensive Assessment of Water Management in Agriculture. Comparative Study of River Basin Development and Management*. International Water Management Institute, Colombo, Sri Lanka.
- Bessah, E., Raji, A. O., Taiwo, O. J., Agodzo, S. K. & Ololade, O. O. 2020 *The impact of varying spatial resolution of climate models on future rainfall simulations in the Pra River Basin (Ghana)*. *Journal of Water and Climate Change* **11** (4), 1263–1283. <https://doi.org/10.2166/wcc.2019.258>.
- Blanc, E. 2012 *The impact of climate change on crop yields in sub-Saharan Africa*. *American Journal of Climate Change* **01** (01), 1–13. <https://doi.org/10.4236/ajcc.2012.11001>.
- Boé, J., Terray, L., Habets, F. & Martin, E. 2008 *Statistical and dynamical downscaling of the Seine basin climate for hydro-meteorological studies*. *International Journal of Climatology* **27**, 1643–1655. <https://doi.org/10.1002/joc>.
- Brink, A. B. & Eva, H. D. 2009 *Monitoring 25 years of land cover change dynamics in Africa: a sample based remote sensing approach*. *Applied Geography* **29** (4), 501–512. <https://doi.org/10.1016/j.apgeog.2008.10.004>.
- Chemnitz, C. & Hoeffler, H. 2011 *Adapting African agriculture to climate change*. *International Journal Rural Development* **45**, 32–35.
- Chemura, A., Schauburger, B. & Gornott, C. 2020 *Impacts of climate change on agro-climatic suitability of major food crops in Ghana*. *PLoS ONE* **15** (6), 1–21. <https://doi.org/10.1371/journal.pone.0229881>.

- Dembélé, M. & Zwart, S. J. 2016 Evaluation and comparison of satellite-based rainfall products in Burkina Faso, West Africa. *International Journal of Remote Sensing* **37** (17), 3995–4014. <https://doi.org/10.1080/01431161.2016.1207258>.
- Dembélé, M., Schaefli, B., Giesen, N. V. D. & Mariéthoz, G. 2020 Suitability of 17 gridded rainfall and temperature datasets for large-scale hydrological modelling in West Africa. *Hydrology and Earth System Sciences* **24**, 5379–5406.
- Epule, T. E., Ford, J. D., Lwasa, S. & Lepage, L. 2017 Climate change adaptation in the Sahel. *Environmental Science and Policy* **75**, 121–137. <https://doi.org/10.1016/j.envsci.2017.05.018>.
- Funk, C., Peterson, P., Landsfeld, M., Pedreros, D., Verdin, J., Shukla, S., Husak, G., Rowland, J., Harrison, L., Hoell, A. & Michaelsen, J. 2015 The climate hazards infrared precipitation with stations – a new environmental record for monitoring extremes. *Scientific Data* **2**, 1–21. <https://doi.org/10.1038/sdata.2015.66>.
- Gornall, J., Betts, R., Burke, E., Clark, R., Camp, J., Willett, K. & Wiltshire, A. 2010 Implications of climate change for agricultural productivity in the early twenty-first century. *Philosophical Transactions of the Royal Society B: Biological Sciences* **365** (1554), 2973–2989. <https://doi.org/10.1098/rstb.2010.0158>.
- Gulacha, M. M. & Mulungu, D. M. M. 2016 Generation of climate change scenarios for precipitation and temperature at local scales using SDSM in Wami-Ruvu River Basin Tanzania. *Physics and Chemistry of the Earth* **100**, 62–72. <https://doi.org/10.1016/j.pce.2016.10.003>.
- Hope, K. R. 2009 Climate change and poverty in Africa. *International Journal of Sustainable Development and World Ecology* **16** (6), 451–461. <https://doi.org/10.1080/13504500903354424>.
- IPCC. 2007 Synthesis report. In: *Synthesis Report. Contribution of Working Groups I, II and III to the Fourth Assessment Report of the Intergovernmental Panel on Climate Change* (Core Writing Team, Pachauri, R. K. & Reisinger, A., eds). IPCC. <https://doi.org/10.1038/446727a>.
- IPCC 2014 Summary for policymakers. In: *Climate Change 2014: Synthesis Report. Contribution of Working Groups I, II and III to the Fifth Assessment Report of the Intergovernmental Panel on Climate Change* (Core Writing Team, Pachauri, R. K. & Meyer, L. A., eds). IPCC, Geneva, Switzerland. <https://doi.org/10.1017/CBO9781139177245.003>.
- Johnson, F. & Sharma, A. 2011 Accounting for interannual variability: a comparison of options for water resources climate change impact assessments. *Water Resources Research* **47** (4). <https://doi.org/10.1029/2010WR009272>.
- Kasei, R. A. 2009 Modelling Impacts of Climate Change on Water Resources in the Volta Basin, West Africa. Rheinischen Friedrich-Wilhelms-Universität Bonn. Available from: http://hss.ulb.uni-bonn.de/diss_onlineelektronisch/publiziert.
- Kasei, R., Diekkrüger, B. & Leemhuis, C. 2010 Drought frequency in the Volta Basin of West Africa. *Sustainability Science* **5** (1), 89–97. <https://doi.org/10.1007/s11625-009-0101-5>.
- Kiros, G., Shetty, A. & Nandagiri, L. 2016 Analysis of variability and trends in rainfall over northern Ethiopia. *Arabian Journal of Geosciences* **9** (451), 1–12. <https://doi.org/10.1007/s12517-016-2471-1>.
- Kjellström, E., Barring, L., Nikulin, G., Nilsson, C., Persson, G. & Strandberg, G. 2016 Production and use of regional climate model projections – a Swedish perspective on building climate services. *Climate Services* **2–3**, 15–29. <https://doi.org/10.1016/j.cliser.2016.06.004>.
- Klassou, K. S. & Komi, K. 2021 Analysis of extreme rainfall in Oti River Basin (West Africa). *Journal of Water and Climate Change* 1–13. <https://doi.org/10.2166/wcc.2021.154>.
- Komi, K., Amisigo, B. A. & Diekkrüger, B. 2016 Integrated flood risk assessment of rural communities in the Oti River Basin, West Africa. *Hydrology* **3** (4), 1–14. <https://doi.org/10.3390/hydrology3040042>.
- Komi, K., Neal, J., Trigg, M. A. & Diekkrüger, B. 2017 Modelling of flood hazard extent in data sparse areas: a case study of the Oti River basin, West Africa. *Journal of Hydrology: Regional Studies* **10**, 122–132. <https://doi.org/10.1016/j.ejrh.2017.03.001>.
- Kunstmann, H. & Jung, G. 2005 Impact of regional climate change on water availability in the Volta Basin of West Africa. In *Regional Hydrological Impacts of Climatic Variability and Change (Proceedings of Symposium S6)*, April 1–11. Available from: papers2://publication/uuid/C9E8B1B8-CEE2-458B-8AF3-9463412A741A.
- Larbi, I., Hountondji, F. C. C., Annor, T., Agyare, W. A., Gathenya, J. M. & Amuzu, J. 2018 Spatio-temporal trend analysis of rainfall and temperature extremes in the Veua Catchment, Ghana. *Climate* **6** (87), 1–17. <https://doi.org/10.3390/cli6040087>.
- Lare, A. R. & Nicholson, S. E. 1994 Contrasting conditions of surface water balance in wet years and dry years as a possible land surface-atmosphere feedback mechanism in the West African Sahel. *Journal of Climate* **7** (5), 653–668.
- Lebel, T., Cappelaere, B., Galle, S., Hanan, N., Kergoat, L., Levis, S., Vieux, B., Descroix, L., Gosset, M., Mougin, E., Peugeot, C. & Seguis, L. 2009 AMMA-CATCH studies in the Sahelian region of West-Africa: an overview. *Journal of Hydrology* **375** (1–2), 3–13. <https://doi.org/10.1016/j.jhydrol.2009.03.020>.
- Li, S., Yang, H., Lacayo, M., Liu, J. & Lei, G. 2018 Impacts of land-use and land-cover changes on water yield: a case study in Jing-Jin-Ji, China. *Sustainability (Switzerland)* **10** (4), 1–16. <https://doi.org/10.3390/su10040960>.
- Lin, H., Jingcai, W., Fan, L., Xie, Y., Jiang, C. & Lipin, S. 2020 Drought trends and the extreme drought frequency and characteristics under climate change based on SPI and HI in the upper and middle reaches of the Huai River Basin, China. *Water* **12** (4), 1100.
- McKee, T. B., Doesken, N. J. & Kleist, J. 1993 The relationship of drought frequency and duration to time scales. In *Proceedings of the 8th Conference on Applied Climatology*. pp. 179–184. <https://doi.org/10.1002/jso.23002>.
- Moriasi, D. N., Arnold, J. G., Liew, M. W. V., Bingner, R. L., Harmel, R. D. & Veith, T. L. 2007 Model evaluation guidelines for systematic quantification of accuracy in watershed simulations. *Transactions of the ASABE* **50** (3), 885–900.
- Muthoni, F. 2020 Spatial-temporal trends of rainfall, maximum and minimum temperatures over West Africa. *IEEE Journal of Selected Topics in Applied Earth Observations and Remote Sensing* **13**, 2960–2973. <https://doi.org/10.1109/JSTARS.2020.2997075>.

- Nhemachena, C., Nhamo, L., Matchaya, G., Nhemachena, C. R., Muchara, B., Karuaihe, S. T. & Mpandeli, S. 2020 Climate change impacts on water and agriculture sectors in Southern Africa: threats and opportunities for sustainable development. *Water* **12** (10), 2673.
- Nicholson, S. E. & Palao, I. M. 1993 A re-evaluation of rainfall variability in the Sahel. Part I. Characteristics of rainfall fluctuations. *International Journal of Climatology* **13** (4), 371–389. <https://doi.org/10.1002/joc.3370130403>.
- Nyatuae, M. & Agodzo, S. 2017 Analysis of extreme rainfall events (drought and flood) over Tordzie watershed in the Volta Region of Ghana. *Journal of Geoscience and Environment Protection* **05** (09), 275–295. <https://doi.org/10.4236/gep.2017.59019>.
- Oguntunde, P. G., Friesen, J., van de Giesen, N. & Savenije, H. H. G. 2006 Hydroclimatology of the Volta River Basin in West Africa: trends and variability from 1901 to 2002. *Physics and Chemistry of the Earth* **31** (18), 1180–1188. <https://doi.org/10.1016/j.pce.2006.02.062>.
- Olesen, J. E., Carter, T. R., Díaz-Ambrona, C. H., Fronzek, S., Heidmann, T., Hickler, T., Holt, T., Minguez, M. I., Morales, P., Palutikof, J. P., Quemada, M., Ruiz-Ramos, M., Rubæk, G. H., Sau, F., Smith, B. & Sykes, M. T. 2007 Uncertainties in projected impacts of climate change on European agriculture and terrestrial ecosystems based on scenarios from regional climate models. *Climatic Change* **81** (Suppl. 1), 123–143. <https://doi.org/10.1007/s10584-006-9216-1>.
- Önöz, B. & Bayazit, M. 2003 The power of statistical tests for trend detection. *Turkish Journal of Engineering and Environmental Sciences* **27** (4), 247–251. <https://doi.org/10.3906/sag-1205-120>.
- Owusu, K. & Waylen, P. 2009 Trends in spatio-temporal variability in annual rainfall in Ghana (1951–2000). *Weather* **64** (5), 115–120. <https://doi.org/10.1002/wea.255>.
- Reilly, J., Tubiello, F., McCarl, B., Abler, D., Darwin, R., Fuglie, K., Hollinger, S., Izaurrealde, C., Jagtap, S., Jones, J., Mearns, L., Ojima, D., Paul, E., Paustian, K., Riha, S., Rosenberg, N. & Rosenzweig, C. 2003 Optimal portfolio choice under a liability constraint. *Climatic Change* **57**, 43–69. <https://doi.org/10.1023/A>.
- Sajikumar, N. & Remya, R. S. 2015 Impact of land cover and land use change on runoff characteristics. *Journal of Environmental Management* **161**, 460–468. <https://doi.org/10.1016/j.jenvman.2014.12.041>.
- Samuelsson, P., Jones, C. G., Willén, U., Ullerstig, A., Gollvik, S., Hansson, U., Jansson, C., Kjellström, E., Nikulin, G. & Wyser, K. 2011 The Rossby Centre Regional Climate model RCA3: model description and performance. *Tellus, Series A: Dynamic Meteorology and Oceanography* **63** (1), 4–23. <https://doi.org/10.1111/j.1600-0870.2010.00478.x>.
- Satgé, F., Defrance, D., Sultan, B., Bonnet, M., Seyler, F., Rouché, N., Pierron, F. & Paturel, J. 2020 Evaluation of 23 gridded precipitation datasets across West Africa. *Journal of Hydrology* **581**, 1–19.
- Seleshi, Y. & Zanke, U. 2004 Recent changes in rainfall and rainy days in Ethiopia. *International Journal of Climatology* **24** (8), 973–983. <https://doi.org/10.1002/joc.1052>.
- Siraj, K. T., Mohammed, A., Bam, S. & Addisu, S. 2013 Long years comparative climate change trend analysis in terms of temperature, coastal Andhra Pradesh, India. *Abhinav National Monthly Refereed Journal of Research in Science & Technology* **2**, 1174–2277.
- Song, W. & Deng, X. 2017 Land-use/land-cover change and ecosystem service provision in China. *Science of the Total Environment* **576**, 705–719. <https://doi.org/10.1016/j.scitotenv.2016.07.078>.
- Suleiman, Y. & Ifabiyi, I. 2015 The role of rainfall variability in reservoir storage management at Shiroro hydropower dam, Nigeria. *AFRREV STECH: An International Journal of Science and Technology* **3** (2), 18–30. <https://doi.org/10.4314/stech.v3i2.2>.
- Teutschbein, C. & Seibert, J. 2012 Bias correction of regional climate model simulations for hydrological climate-change impact studies: review and evaluation of different methods. *Journal of Hydrology* **456–457**, 12–29. <https://doi.org/10.1016/j.jhydrol.2012.05.052>.
- Thom, H. C. S. 1958 Monthly weather review. *Monthly Weather Review* **86** (4), 117–122. <https://doi.org/10.1126/science.26.653.25>.
- Travis, W. R. 2016 Agricultural impacts: mapping future crop geographies. *Nature Climate Change* **6** (6), 544–545. <https://doi.org/10.1038/nclimate2965>.
- Tschakert, P., Sagoe, R., Ofori-Darko, G. & Codjoe, S. N. 2010 Floods in the Sahel: an analysis of anomalies, memory, and anticipatory learning. *Climatic Change* **103** (3–4), 471–502. <https://doi.org/10.1007/s10584-009-9776-y>.
- Twisa, S. & Buchroithner, M. F. 2019 Seasonal and annual rainfall variability and their impact on rural water supply services in the Wami River Basin, Tanzania. *Water* **11** (2055), 1–18.
- Wheeler, T. & Von Braun, J. 2013 Climate change impacts on global food security. *Science* **341** (6145), 508–513. <https://doi.org/10.1126/science.1239402>.
- Woldesenbet, T. A., Elagib, N. A., Ribbe, L. & Heinrich, J. 2017 Hydrological responses to land use/cover changes in the source region of the Upper Blue Nile Basin, Ethiopia. *Science of the Total Environment* **575**, 724–741. <https://doi.org/10.1016/j.scitotenv.2016.09.124>.
- Yang, J., Xie, B., Zhang, D. & Tao, W. 2021 Climate and land use change impacts on water yield ecosystem service in the Yellow River Basin, China. *Environmental Earth Sciences* **80** (3), 1–12. <https://doi.org/10.1007/s12665-020-09277-9>.
- Yue, S., Pilon, P. & Cavadias, G. 2002 Power of the Mann–Kendall and Spearman’s rho tests for detecting monotonic trends in hydrological series. *Journal of Hydrology* **259**, 254–271.
- Zhang, Q., Sun, P., Li, J., Xiao, M. & Singh, V. P. 2015 Assessment of drought vulnerability of the Tarim River basin, Xinjiang, China. *Theoretical and Applied Climatology* **121** (1–2), 337–347.

First received 26 September 2021; accepted in revised form 5 February 2022. Available online 21 February 2022